

**Chapter V**  
**Results and Discussion**  
**Part C**

*Influence of polar substituent in the central bent core unit of four ring bent liquid crystals on mesomorphism.*

## 5.1. Introduction:

The discovery of spontaneous polarity [1] and chirality [2] in smectic phases of bent shaped molecules has stimulated a new area of interest in the field of soft material science [3], which attracts both physicists and chemists due to their special characteristics like supramolecular chirality, ferro- and anti-ferro electricity, electro-optic switching and exotic phases. The prerequisite for attaining polar order and chirality in any of the materials is that the individual molecule should possess a bent shape in the central core and form smectic layers in which the molecular planes tilted, resulting in spontaneously chiral architecture. The molecular bend in these materials can be achieved using substituted central ring systems [3], including unsymmetrical groups such as the 3,4'-disubstituted biphenyl unit [4], or by the use of linking groups, such as esters [5] or short aliphatic chains [6]. Recently we reported the fluid smectic LC phases with spontaneously growing chiral and polar layers (SmCP phases) including the polarization splay modulated and layer undulated (PMLU) B<sub>7</sub>/B<sub>1Rev/Tilted</sub> phases variants in four ring bent core systems [7]. The four ring molecule possesses two OH groups in two wings, located in unsymmetrical positions, which deviates significantly from the typical symmetrical and/or V-shape of other bent core molecules. Further we observed helical structures in these four ring achiral systems and this phenomenon is the strong evidence that the origin of the chirality in this system viz. ferro/antiferroelectricity and twisted structures is related to the twist conformation of these molecules. The modification of angular 3,4'-disubstituted biphenyl unit [8] with the introduction of an ester linkage viz., COO moiety between the phenyl units, reduction of phenyl rings and proper choice of a substituent and its position in the central core leads to structural variation of polar groups in bent core molecules and hence can promote a broad range of interesting variations [7] in their mesogenic properties. The bent core unit viz. **3,4'-disubstituted biphenyl** had been successfully demonstrated as a central core unit in five, six and seven ring molecules exhibiting several variants of banana phases. The majority of the reported four-ring bent-core compounds are non mesomorphic [9-13]. However Hird et al reported fluoro substituted bent-core compounds exhibiting monotropic nematic phase with chiral domains. The earlier reported four-ring molecules with a biphenyl moiety in the wing possessing fluoro substituents on the central ring viz. [(S)-1-methylheptyl-4-[2,3,4-trifluoro-5-(4'-dodecyloxy-biphenyl-4-ylcarbonyloxy)-phenylcarbonyloxy] benzoate] exhibited conventional SmA, ferro-, ferri-, and antiferroelectric SmC phases resulting from the molecular chirality and not due to the bent shape [14]. Weissflog et al recently reported asymmetric achiral four-ring bent-core mesogens derived from N-benzoylpiperazine and only few of them found to exhibit only calamitic phases. The introduction of a substituent in the side wings of the molecules also does not promote the mesomorphism [13]. They reported polar structures under the

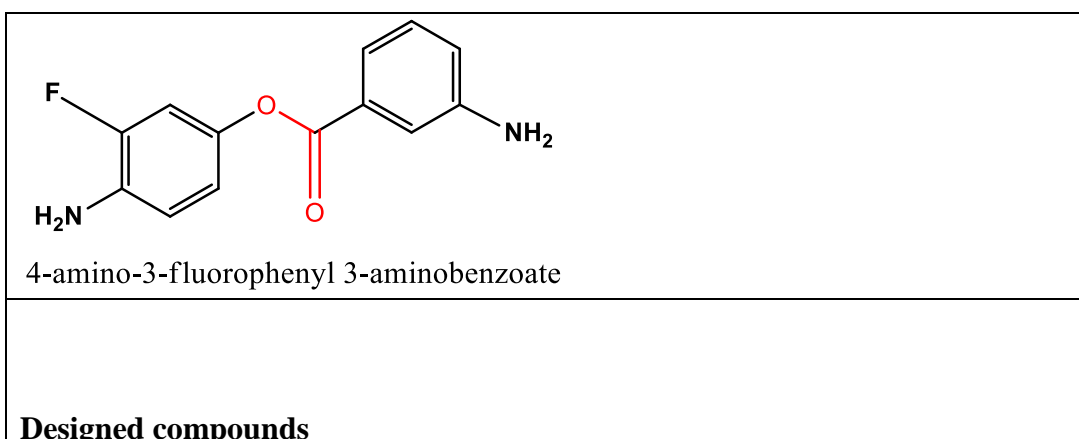
influence of electric field in these four-ring bent-core compounds exhibiting calamitic type smectic phases. Moreover they also exhibited switchable smectic I phase the first example of non-chiral ferroelectric SmI phase ( $\text{SmIP}_F$ ), which is attributed due to bent shape of the molecules. None of these four-ring compounds are found to spontaneously exhibit typical banana phases ( $\text{SmAP}$ ,  $\text{SmCP}$ ) because of weak steric interactions between the aromatic cores. Kang et al [14] reported a four-ring oxadiazole derivative exhibiting nematic-SmC-Bx phase variant. The Bx phase is found to be uniaxial, exhibited randomly distributed domains of opposite handedness and under the influence of electric field transformed to a homochiral  $\text{SmC}_A\text{P}_F$  phase with antiferroelectric response. The liquid crystalline phase behaviour of bent or banana-shaped compounds is dependent upon several factors, namely the size of the molecule and the number of aromatic rings, the position as well as the magnitude of the bent angle, the size, number, position and nature of the substituents, the nature and direction of linkage groups and the length and nature of the terminal alkyl chains. In general, any minor change in these structural elements leads to drastic changes in the phase behaviour. One of the important aspects is the nature and size of the substituent in the central core, which largely influences the mesophase behaviour [15-19]. Several research groups studied the influence of the lateral substituents on the mesophase behaviour either in the central core or the outer rings [15-25]. However, the introduction of a small substituent into the central 1,3-phenylene ring leads to the possibility of synthesising new mesogens with novel banana phases [22-27]. Moreover, it was found that mesophase behaviour is much more strongly influenced by substituents at the central core than by these at the outer ring [28-31]. Rich variety of banana phases was discovered by introducing lateral substituents in the central ring as well as side wings. In case of lateral substitution three major factors are involved depending on the size and polarity of the substituents namely inter- and intra molecular forces of attraction, repulsion of the substituents and the position of the substitution. These factor influence molecular conformation. Molecular conformation effects on molecular packing and vice versa. Consequently, lateral substitution has an impact on the liquid crystalline state, i.e. on the liquid crystalline behaviour. Systematic study of banana substance classes one by one, may advance understanding of this subject.

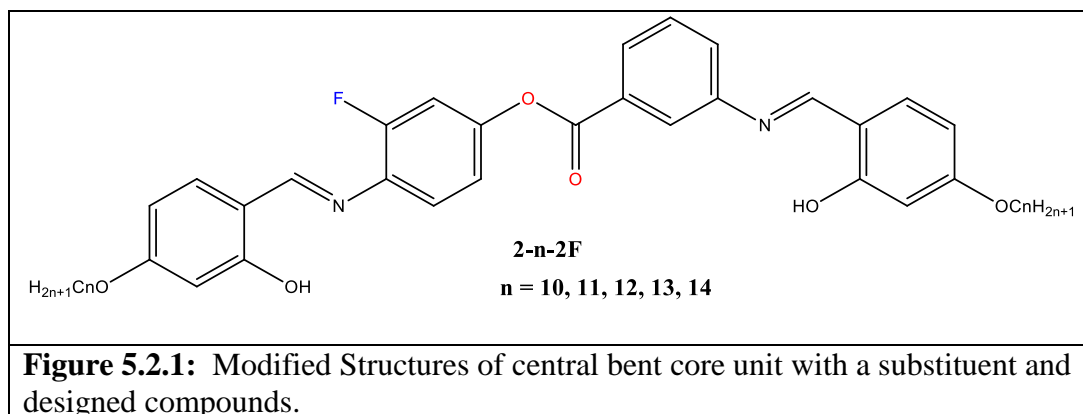
## **5.2. Effect of Fluoro substituents:**

The fluoro substituent in organic compounds is regarded as so interesting because of the combination of polar and steric effects, and the great strength of the C–F bond which confers stability on fluoro-substituted compounds. Fluorine has the highest electro-negativity of all the elements (3.98), and hence as a substituent confers a high dipole moment on the C–F bond. In an aliphatic or alicyclic environment the dipole moment is relatively large, e.g., 1.85 D in fluoromethane, however, in an aromatic environment the mesomeric effect causes a reduction in

dipole moment, e.g., 1.50 D for fluorobenzene. Despite the high polarity, the fluoro substituent has a low polarizability which confers low intermolecular dispersion interactions. The fluoro substituent is the smallest, after hydrogen, of all possible substituents, and like hydrogen it is monoatomic. So although a fluoro substituent obviously causes a steric effect, the size influence is not too drastic, which enables it to be usefully incorporated into parent molecules for beneficial modification of properties. Lateral substituents, particularly fluoro, are frequently employed in liquid crystal structures to modify melting point, liquid crystal transition temperatures and mesophase morphology and to modify the physical properties of liquid crystals to enable their use in applications. Fluoro substituents have been so successfully and usefully incorporated into liquid crystal molecules because of the combination of small size and high polarity [32-34] and because the high strength of the C–F bond confers excellent stability. The relatively small size of a fluoro substituent means that it does not unduly alter the necessary stylized structure, which helps to maintain the existing liquid crystalline nature of the compound. However, the important attributes of the fluoro substituent discussed above, ensures that subtle, but significant, modifications are frequently encountered in respect of melting point, mesophase morphology, transitions temperatures, and the many essential physical properties of liquid crystals, such as optical, dielectric, and visco-elastic properties. Such alterations to the attributes of liquid crystals are of great significance in terms of fundamental academic structure–property relationships, and crucial to the development of commercially-successful liquid crystal displays. The structure of this series of compound is shown in **Figure 5.2.1**.

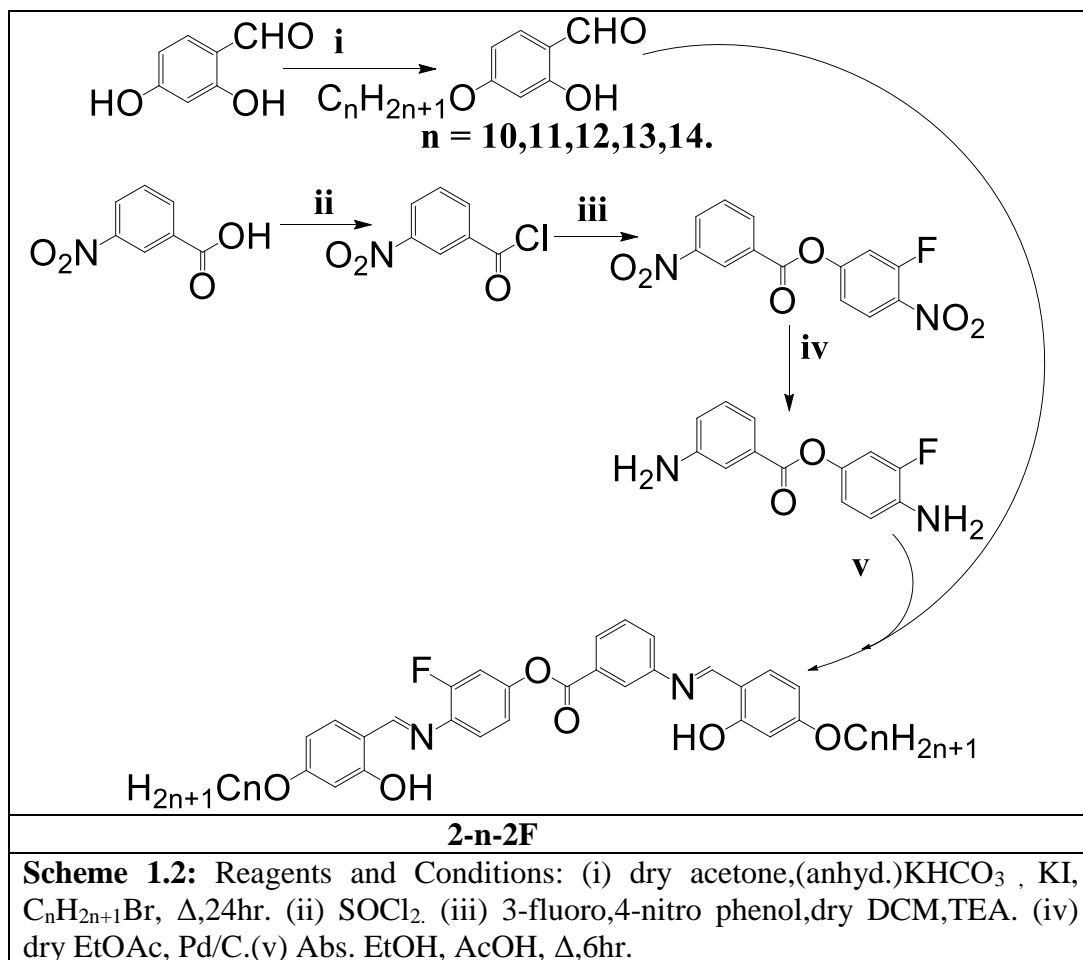
#### Modified Structures of central bent core unit with a substituent





### 5.3. Synthesis:

The starting material in the present study 4-n-alkyloxysalicylaldehyde was prepared by Williamson etherification of 2,4-dihydroxybenzaldehyde with appropriate n-alkyl bromide. The central bent core moiety 4-amino-3-fluorophenyl-3-aminobenzoate was prepared as follows. 3-nitrobenzoic acid was converted into its acyl chloride followed by condensation with 3-fluoro-4-nitrophenol using phase transfer reaction. The resultant 4-amino-3-fluorophenyl-3-aminobenzoate was subjected to 10% Pd-C catalysed reduction to get the desired di-amino bent-core compound. The condensation of 4-n-alkyloxy salicylaldehyde with 4-amino-3-fluorophenyl-3-aminobenzoate in presence of a few drops of glacial acetic acid yielded the target bent shaped compounds. To avoid the formation of side products, the precipitated compounds were filtered when the solution was hot to yield the pure compounds. The compounds were further recrystallized repeatedly to get the pure samples [5(a)]. The synthetic scheme for synthesis of the series of compound is presented in **Scheme 1.2**. The formation of all of the compounds was confirmed by <sup>1</sup>HNMR and IR spectroscopy and the purity was established by elemental analysis. The other homologues with n = 10,11,12,13,14 were also synthesized following the same procedure and characterized. The liquid-crystalline behaviour of the synthesised compounds had been investigated by optical microscopy and differential scanning calorimetry (DSC). The detailed synthesis, FT-IR, <sup>1</sup>H-NMR and elemental analysis of all the compounds of the homologous series **2-n-2F** is presented in chapter III.



#### 5.4. Mesomorphic properties:

The transition temperatures, enthalpies and entropies associated with the phase transitions of all the compounds of the homologous series **2-n-2F** ( $n = 10$  to  $14$ ) as a function of number of the carbon atoms in the terminal alkyl chains obtained from DSC at a scan rate of  $5^{\circ}\text{C min}^{-1}$  in the second heating and first cooling scans are presented in **Table 5.4.1**. All compounds of the homologous series exhibit banana liquid crystalline behaviour over a moderate temperature region. The calorimetric study on a representative compound **2-14-2F** is presented here. The differential scanning calorimetric thermogram of **2-14-2F** is presented in **Figure 5.4.3**.

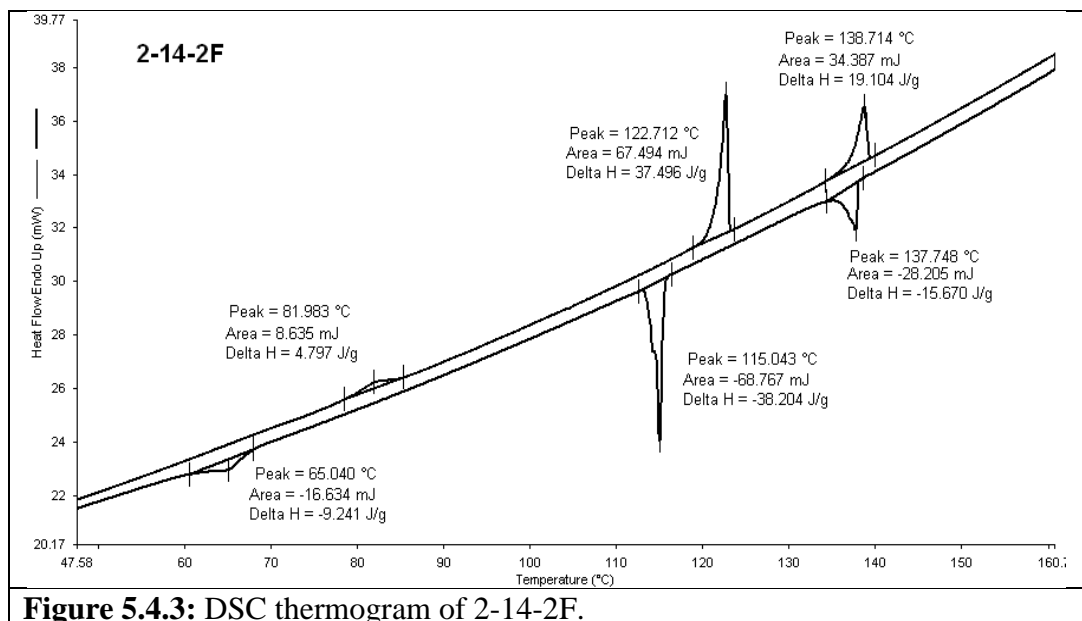


**Figure 5.4.3:** DSC thermogram of 2-14-2F.

**Table 5.4.1:** Phase transition temperatures ( $^{\circ}\text{C}$ ) of the compounds **2-14-2F**, recorded for second heating (first row) and second cooling (second row) cycles at  $5^{\circ}\text{C}/\text{min}$  from DSC. The enthalpies ( $\Delta H$  in  $\text{kJ}/\text{mol}$ ) and entropies ( $\Delta S$  in  $\text{J}/\text{mol}/\text{K}$ ) respectively are presented in parentheses.

Compound	K- K1	K1-B7	B7-I
<b>2-14-2F</b>	81.9(4.22, 11.9)	122.7(32.95, 83.29)	138.7(16.79, 40.79)
	65.0(8.12, 24.02)	115.0(33.57, 86.54)	137.7(13.78, 33.53)
<b>2-13-2F</b>	114.0 (26.6, 68.9)	121.9 (17.0, 43.0)	138.7 (10.6, 25.8)
	62.6 (5.6, 16.9)	114.0 (21.0, 54.2)	137.8 (10.1, 24.6)
<b>2-11-2F</b>	107.9 (34.6, 91.0)	121.7 (30.5, 77.3)	137.7 (12.8, 31.3)
	50.6 (14.0, 43.4)	113.6 (32.5, 84.1)	137.3 (7.2, 17.6)
<b>2-10-2F</b>	92.9 (4.2, 11.5)	122.1 (13.2, 33.5)	137.2 (5.7, 14.0)

The observed optical textures exhibited by a representative compound **2-14-2F** are presented in **Figure 5.4.4**. Upon very slow cooling the isotropic liquid, compounds **2-14-2F** exhibited developable domains (**Figure 5.4.4a**) and telephone-wire like spiral filaments (**Figure 5.4.4b** and **c**), circular domains, and banana leaf-like domains. The developable circular domain-like textures resemble the B7 phases. The growth of telephone-wire like spiral filament textures has been widely related to the existence of smectic undulated phases [5, 35-37]. The colourful developable domains with dark extinction crosses coinciding with the

direction of polariser and analyser, some with equidistant stripes and checkerboard patterns [35,36,38]. However recent investigations based on high resolution X-ray studies revealed that such type of textures are exhibited by 2D modulated smectic phases of bent core molecules based on locally ferroelectric layering and spontaneous splay of the polarization. Based on polarization splay modulation (either syn- or anti-order), slopes of undulated layers and layer continuity versus layer discontinuity at the intervening defects twelve different phases are proposed. Only some of the phase structures had been realized till now. The textural features of the compounds in the present work (**2-14-2F**) resemble the textures observed in compounds exhibiting 2D polarization splay modulated layer undulated B7/B1<sub>RevTilted</sub> phases [5,35-37].

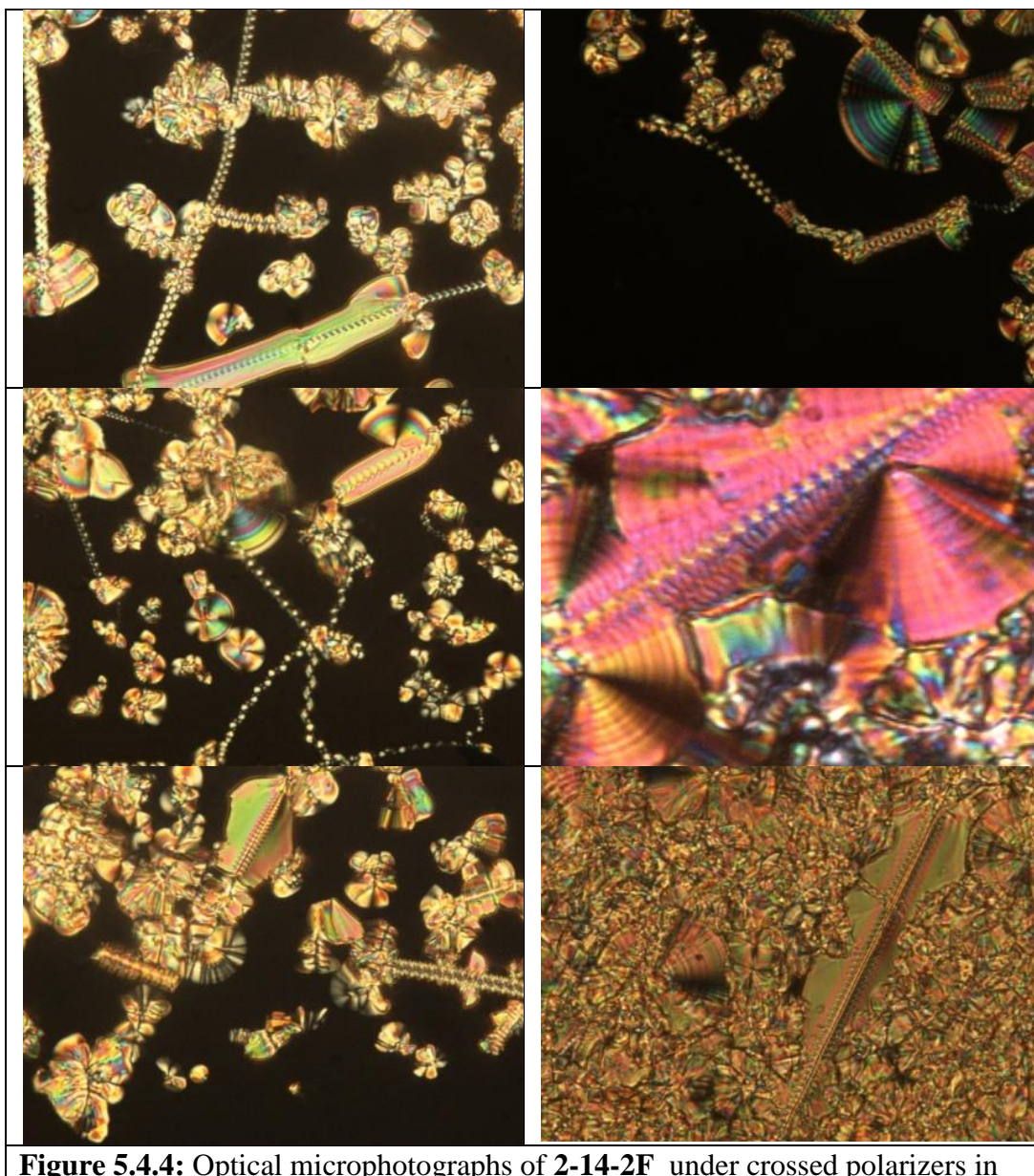
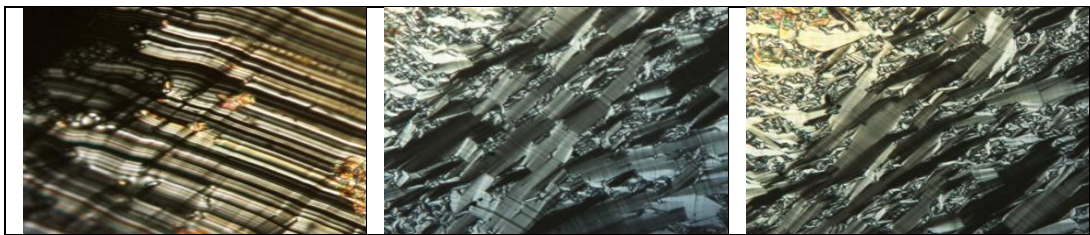


**Figure 5.4.4:** Optical microphotographs of **2-14-2F** under crossed polarizers in

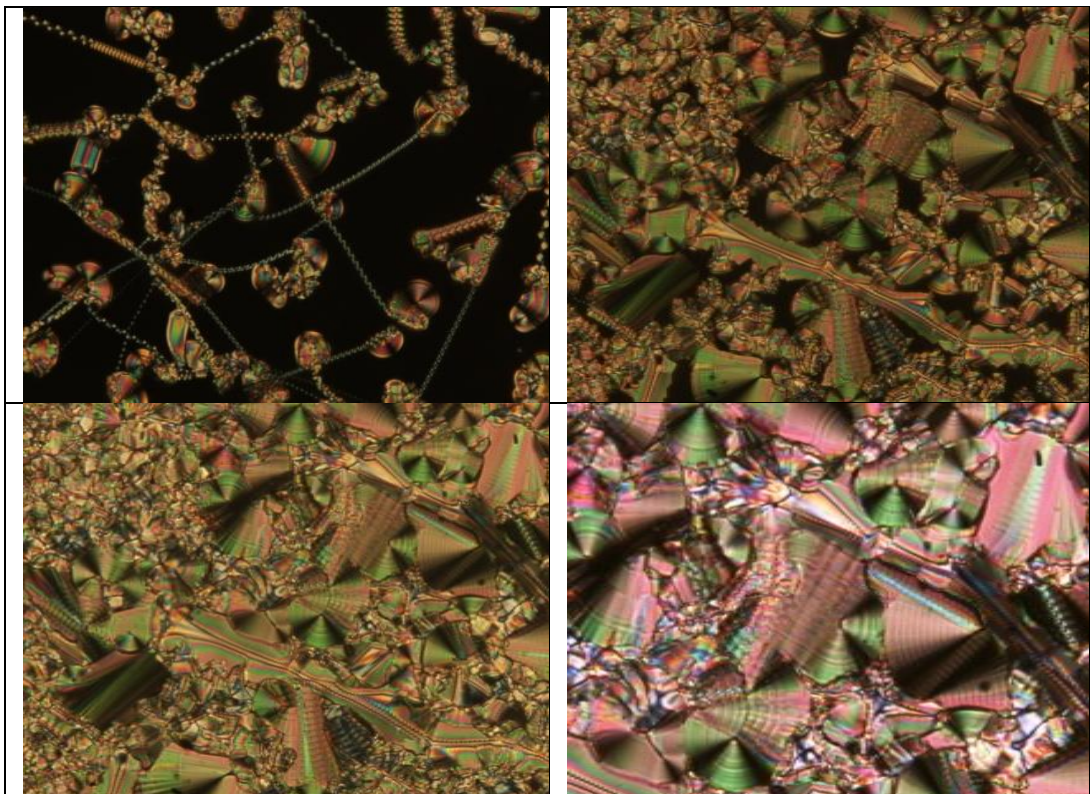


different regions (a) developable domains at  $T = 135^{\circ}\text{C}$ , (b) telephone wire like spiral texture and checkerboard patterns  $T = 132^{\circ}\text{C}$ , (c) circular domains and spiral texture with banana leaf like  $T = 125^{\circ}\text{C}$ , (d) developable domains as well as spiral textures  $T = 122^{\circ}\text{C}$ , (e) banana leaf like textures  $T = 118^{\circ}\text{C}$ , and (f) transition to Cr phase  $T = 116^{\circ}\text{C}$ .

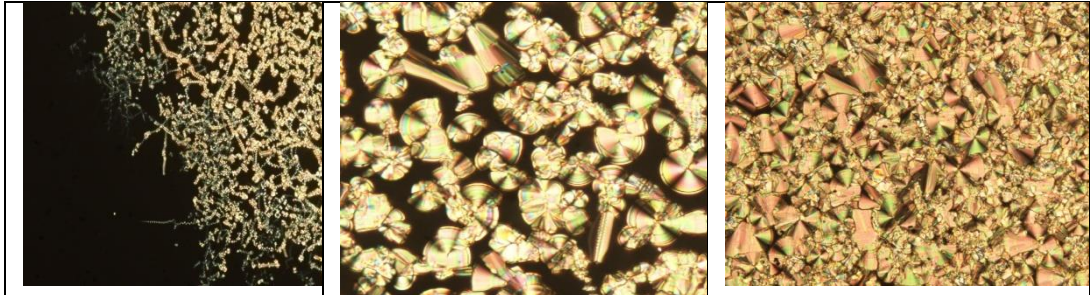
Uncovered free-drop droplets exhibited a fingerprint texture of stripes in focal conic fans (**Fig. 5.4.5**) similar to that found in homeotropic (freely suspended film) B7 preparations [36].



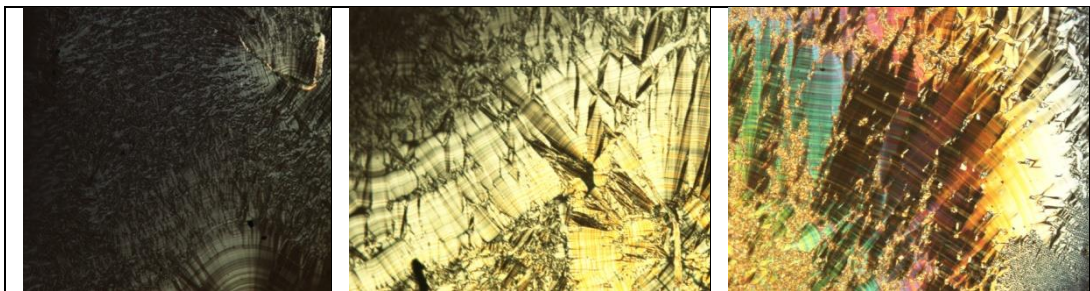
**Figure 5.4.5:** Optical microphotographs of **2-11-2F** of an uncovered drop of B7 phase at  $T = 135^{\circ}\text{C}$ ,  $130^{\circ}\text{C}$  and  $120^{\circ}\text{C}$  respectively.



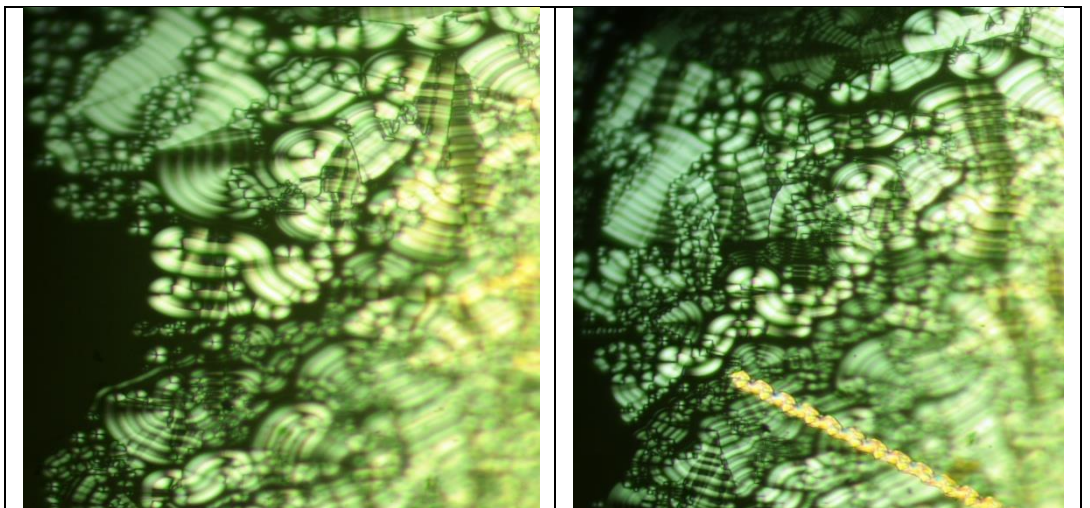
**Figure 5.4.6:** Optical microphotographs of **2-11-2F** under crossed polarizers in different regions.



**Figure 5.4.7:** Optical microphotographs of **2-12-2F** under crossed polarizers in different regions (a) telephone wire like spiral texture at  $T = 135^{\circ}\text{C}$  (b) developable domains at  $T = 132^{\circ}\text{C}$ , (c) circular domains with banana leaf like  $T = 122^{\circ}\text{C}$ .

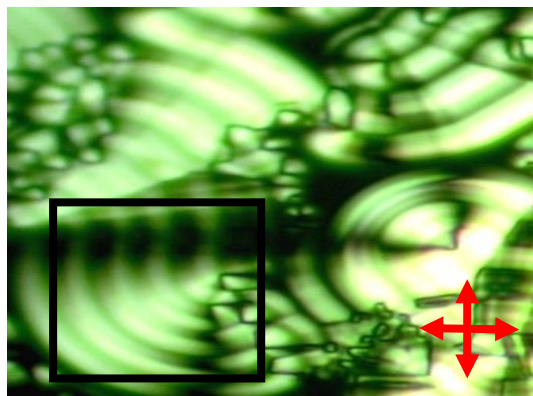


**Figure 5.4.8:** Optical microphotographs of **2-13-2F** of an uncovered drop of B7phase at  $T = 138^{\circ}\text{C}$ ,  $129^{\circ}\text{C}$  and  $118^{\circ}\text{C}$  respectively.

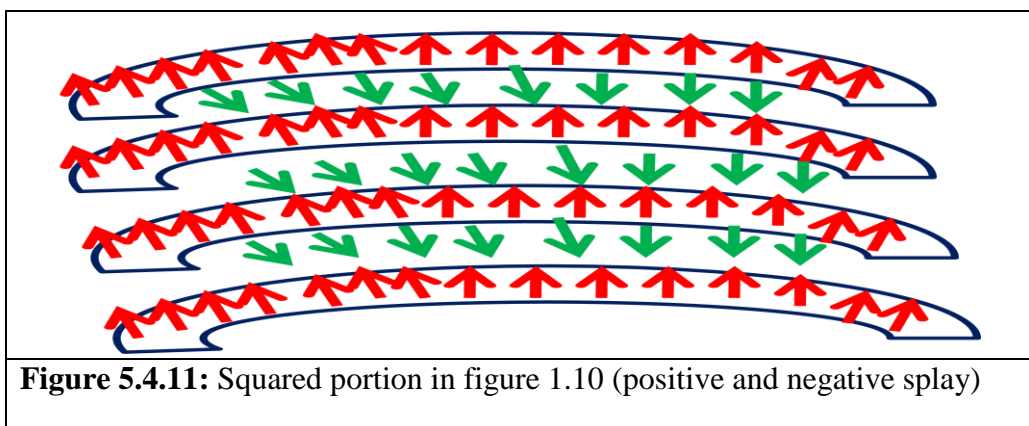


**Figure 5.4.9:** Optical microphotographs of **2-14-2F** of an uncovered drop of B7phase at  $T = 137^{\circ}\text{C}$ ,  $132^{\circ}\text{C}$  respectively.





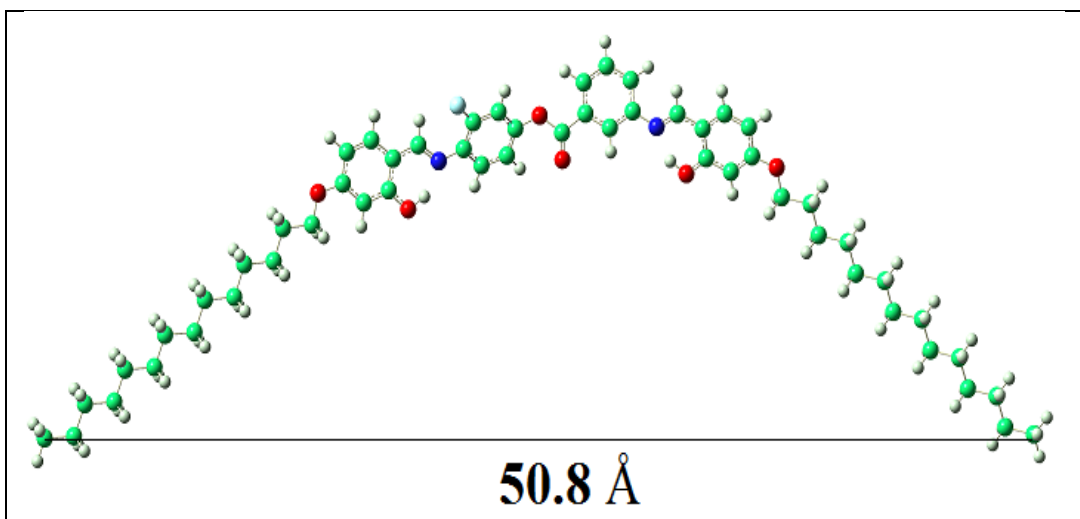
**Figure 5.4.10:** Myelinic domains observed between crossed polarisers in a free drop of B7 in 2-14-2F about 5° below I-B7 transition temperature. The pattern is interpreted as splay-bend regions.



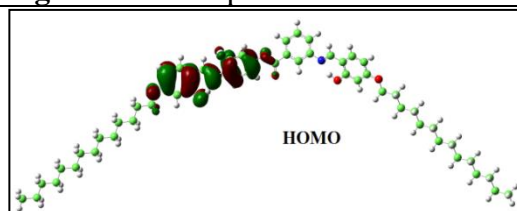
**Figure 5.4.11:** Squared portion in figure 1.10 (positive and negative splay)

### 5.5. Density Functional theory study:

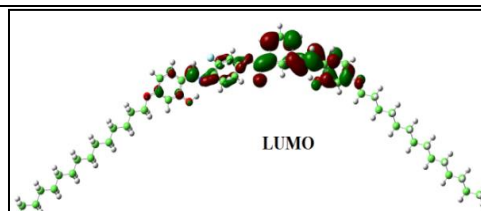
As suitable X-ray quality crystal could not be grown, quantum chemical calculation based on density functional theory (DFT) has been performed to investigate the electronic structure of the 2-14-2F (**Figure 5.5.12**). Full geometry optimization has been carried out without imposing any constrain with the Gaussian 09 program package [41]. Spin-restricted DFT calculation has been carried out in the framework of the generalized gradient approximation (GGA) using Becke3-Lee-Yang-Parr exchange-correlation functional i.e. B3LYP [40, 41] hybrid functional and 6-31G (d, p) basis set.



**Figure 5.5.12:** Optimised molecular structure of 2-14-2F.

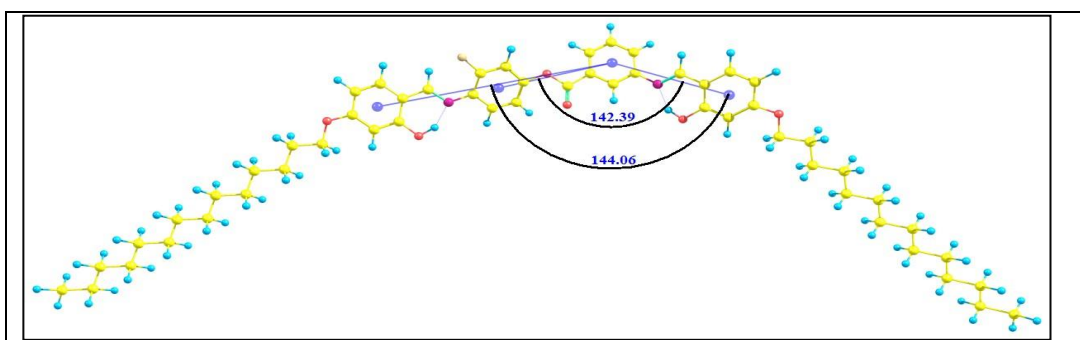


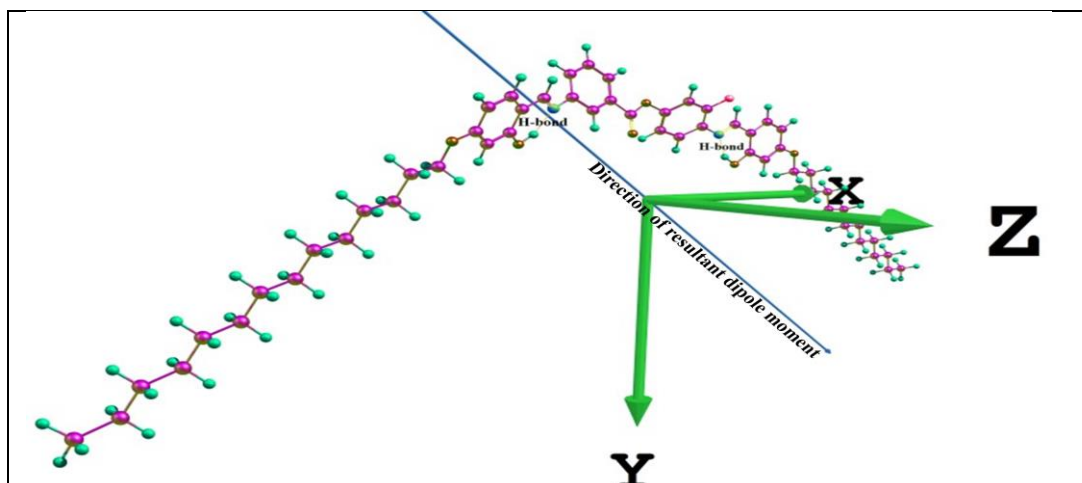
**Figure 5.5.13:** HOMO of 2-14-2F.



**Figure 5.5.14:** LUMO of 2-14-2F.

The 3-D iso-surface plots of the highest occupied molecular orbital (HOMO) and lowest unoccupied molecular orbital (LUMO) of the complex are shown (figures 15 and 16). The HOMO and LUMO energies are calculated to be  $-5.468\text{eV}$  and  $-1.733\text{ eV}$ , respectively,  $\Delta E= 3.734\text{ eV}$ . The HOMO–LUMO energy separation can be used as a measure of kinetic stability of the molecule and could indicate the reactivity pattern [42, 43]. A large HOMO–LUMO gap implies a high-kinetic stability and low chemical reactivity, because it is energetically unfavourable to add electrons to a high lying LUMO or to extract electrons from a low-lying HOMO [43]. The HOMO–LUMO energy gap of  $3.734\text{ eV}$  suggests that the compound is fairly stable.





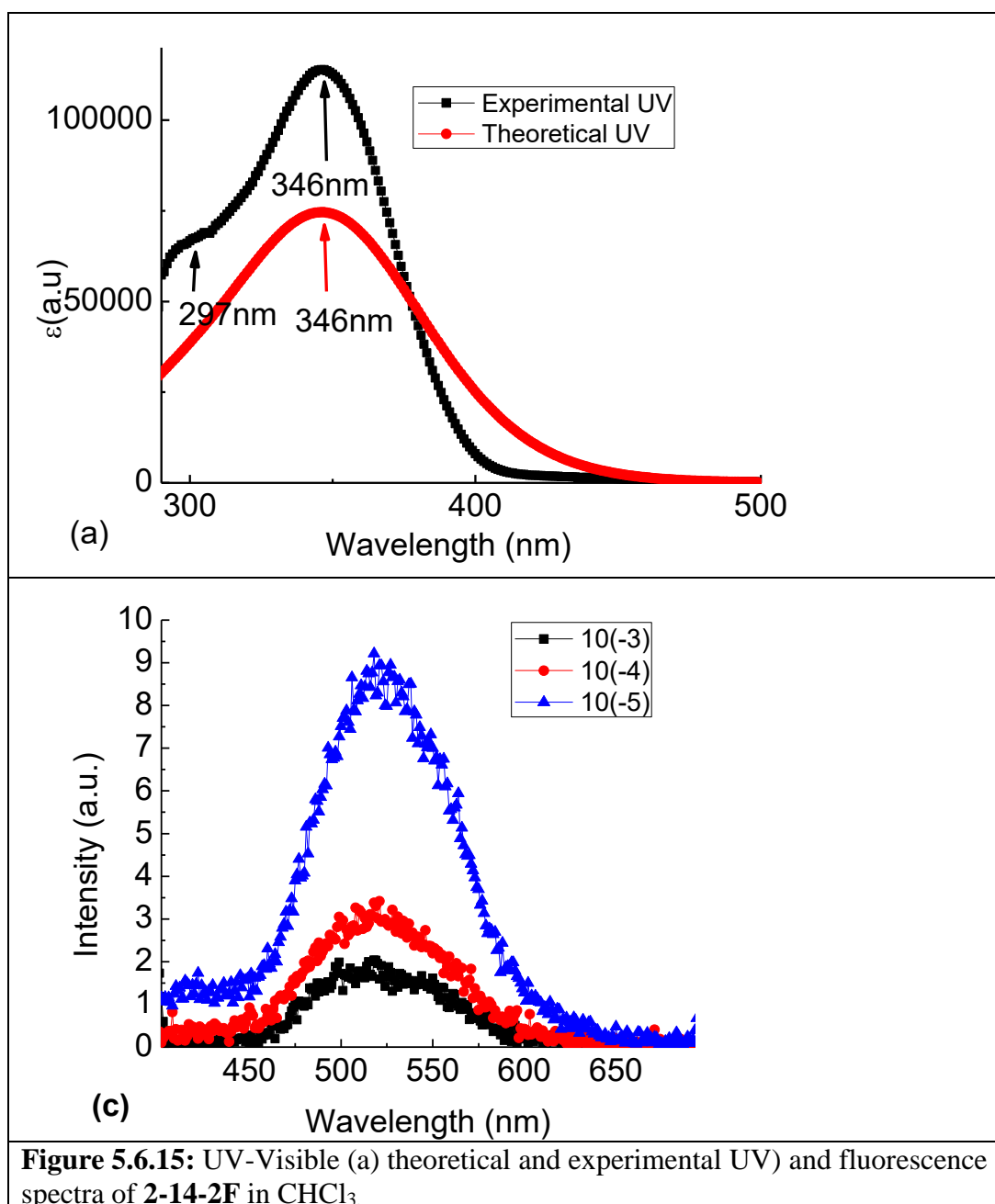
Basis set used	Energy (a.u.)	Dipole moment (Debye)				Bend angle (degree)	Molecular length(Å)
		$\mu_x$	$\mu_y$	$\mu_z$	$\mu_{\text{resultant}} = (\mu_x^2 + \mu_y^2 + \mu_z^2)^{1/2}$		
6-31G(d)	-2801	1.84	1.53	0.15	2.40	143	50.8

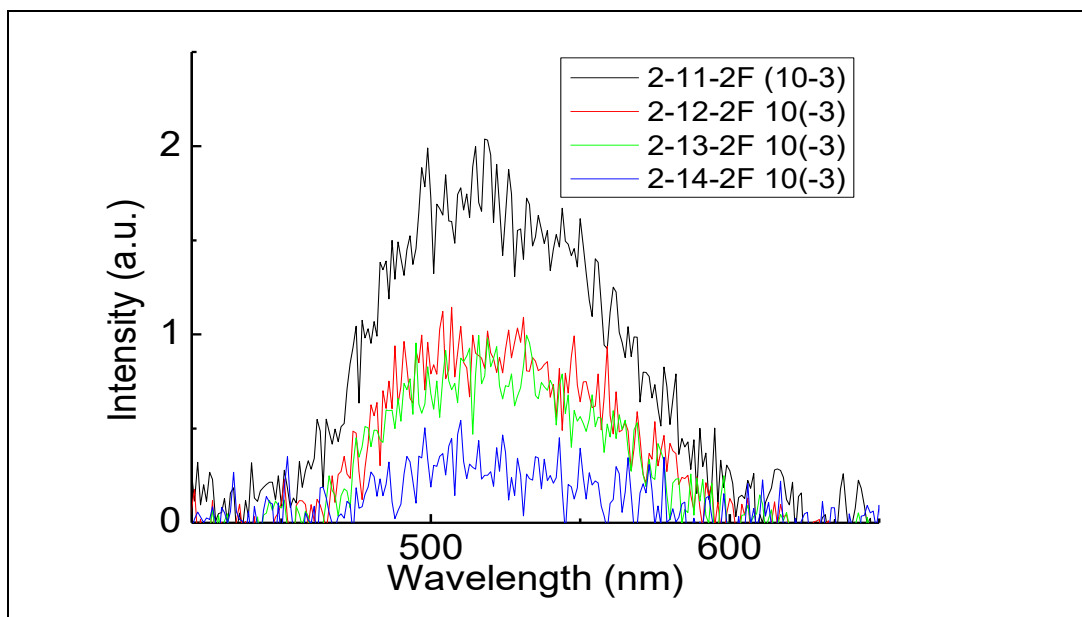
### 5.6. Absorption and emission spectral analysis:

The UV absorption and fluorescence spectroscopic properties of compound **2-14-2F** in solution were studied in various solvents of different concentrations to obtain information regarding absorption and emission maxima, and the Stokes shift of fluorescence. The compounds exhibited similar absorptions with absorption peaks at 346 nm (3.58 eV for 2-14-2F,  $\epsilon \sim 114116 \text{ Lmol}^{-1}\text{cm}^{-1}$ ). These absorption band with large molar absorption coefficients reflects the  $\pi$ - $\pi^*$  transition of the highly  $\pi$ -conjugated system having the substituted phenyl benzoate unit as the core. The theoretical UV-visible study was performed by density functional theory method and it is seen that the compound **2-14-2F** exhibited similar absorption with absorption peak at 346 nm but molar extinction coefficient differs because one is performed in gaseous state and the other in solution. Additionally, we investigated the fluorescence spectrum to observe the characteristic features of the excited states of **2-14-2F**.

The fluorescence emission spectra of these compounds were examined in chloroform solution (conc.  $10^{-3}$ ,  $10^{-4}$  and  $10^{-5} \text{ M}$ ) and it was found that both exhibited strong fluorescence on excitation at 350 nm. The emission peak at  $\lambda_{\text{em}} = 520 \text{ nm}$  (2.38 eV) for compound 2-14-2F, with a large Stokes shift  $\lambda_S$  of the order of  $\lambda_S = 170 \text{ nm}$  (1.20 eV) was attributed to the formation of intermolecular excimers. This Stokes shift, which reflects the structural relaxation of the excited

molecule, is significantly larger than in reported push-pull systems exhibiting liquid crystal behaviour,[31] indicating that the molecular conformation changes upon excitation. The plots of the fluorescence spectra at different concentrations show that the relative intensity of the peak at 520 nm gradually increases with dilution,(**Figure 5.6.15(c)**). The fluorescence spectra of the synthesized homologous series were examined in chloroform solution at  $10^{-3}$  M concentration. It reveals that there is no apparent shift of emission wavelength but the relative intensity of the emission peak decreases with increase in chain length (**Figure 5.6.16**).

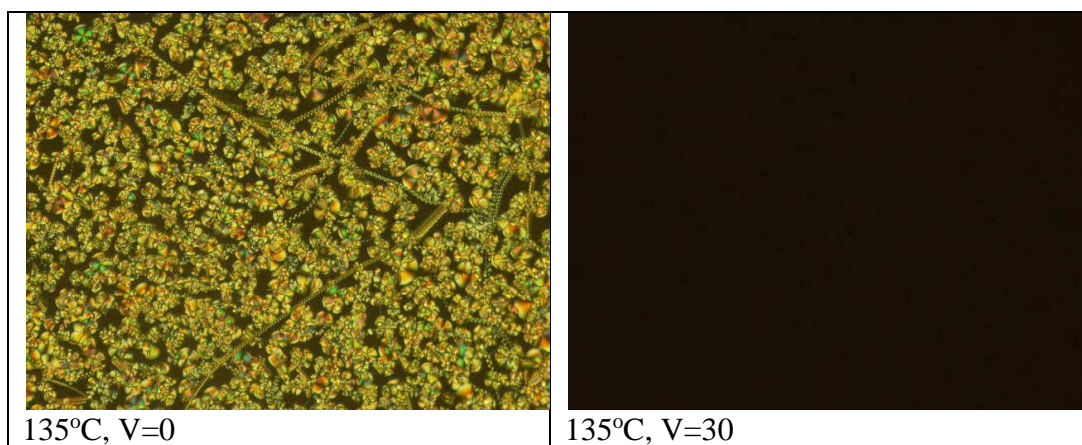




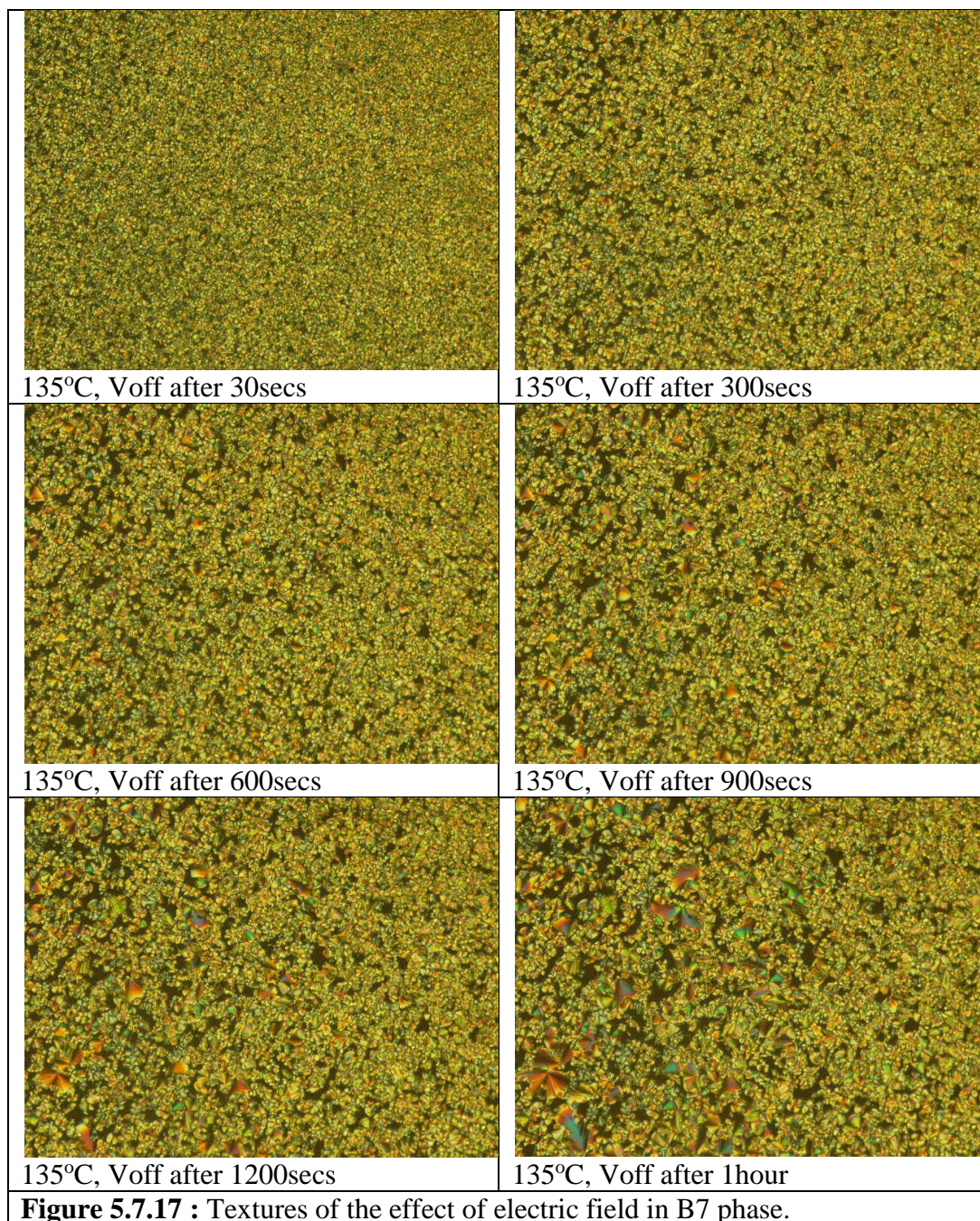
**Figure 5.6.16 :** Fluorescence spectra of the series at  $10^{-3}$  M concentration chloroform solution.

### 5.7. Electro-optical study:

The sample 2-14-2F was filled in  $5\mu\text{m}$  cell in the isotropic phase and upon cooling down to  $135^\circ\text{C}$ , when there was full growth of B7 texture, electric field of 30V was applied. It is seen that the texture becomes optically isotropic indicating the homeotropic alignment of molecules. Upon withdrawing of electric field, the texture retains its original position with due course of time (**Figure 5.7.17**).







### 5.8. Conclusion:

The four ring bent shaped molecules with fluorine substituent at the phenyl ring was successfully synthesized. Polarising optical microscopy study of the homologous series shows that the compounds exhibit B7 texture. The growth of telephone-wire like spiral filament textures has been widely related to the existence of smectic undulated phases. Uncovered free-drop droplets exhibited a fingerprint texture of stripes in focal conic fans similar to that found in homeotropic (freely suspended film) B7 preparations.



Electro-optical study reveals that the texture becomes optically isotropic upon application of small field (30 V) and regenerates back on removal of the field with due course of time.

### References:

[1] T. Niori, T. Sekine, J. Watanabe, T. Furukawa and H. Takezoe, *J. Mater. Chem.*, **6**, 1231–3, (1996).

[2] D. R. Link, G. Natale, R. F. Shao, J. E. MacLennan, N. A. Clark, E. Korblova and D. M. Walba, *Science*, **278**, 1924–1927, (1997).

[3] (a) H. Takezoe and Y. Takanishi, *Jpn. J. Appl. Phys.*, **45**, 597–625, (2006); (b) R. A. Reddy and C. Tschierske, *J. Mater. Chem.*, **16**, 907–961, (2006); (c) M. B.

- Ros, J. L. Serrano, M. R. de la Fuente and C. L. Folcia, *J. Mater. Chem.*, **15**, 5093–5098, (2005); (d) C. Tschierske and G. Dantlgraber, *Pramana*, **61**, 455–481, (2003); (e) G. Pelzl, S. Diele and W. Weissflog, *Adv. Mater.*, **11**, 707–724, (1999).
- [4](a) D. Shen, S. Diele, I. Wirth and C. Tschierske, *Chem. Commun.*, 2573–2574, (1998); (b) D. Shen, A. Pegenau, S. Diele, I. Wirth and C. Tschierske, *J. Am. Chem. Soc.*, **122**, 1593–1601, (2000).
- [5] R. A. Reddy, U. Baumeister, C. Keith, H. Hahn, H. Lang and C. Tschierske, *Soft Mater*, **3**, 558–570, (2007).
- [6] S. W. Choi, M. Zennyoji, Y. Takanishi, H. Takezoe, T. Niori and J. Watanabe, *Molecular Crystals and Liquid Crystals*, **328**, 185–192, (1999).
- [7] (a) R. Deb, R. K. Nath, M. K. Paul, N. V. S. Rao, F. Tuluri, Y. Shen, R. Shao, D. Chen, C. Zhu, I. I. Smalyukh and N. A. Clark, *J. Mater. Chem.*, **20**, 7332–7336, (2010); (b) D. K. Yoon, R. Deb, D. Chen, E. Korblova, R. Shao, K. Ishikawa, N. V. S. Rao, D. M. Walba, I. I. Smalyukh and N. A. Clark, *Proc. Nat. Acad. Sci.*, **107**, 21311–21315, (2010).
- [8] F. C. Yu and L. J. Yu, *Chem. Mater.*, **18**, 5410, (2006).
- [9] J. H. Wild, K. Bartle, M. O’Neill, S. M. Kelly and R. P. Tuffin *Liq. Cryst.*, **33**, 635, (2006).
- [10] S. Sokolowski, H. Dehne, W. Weissflog, unpublished.
- [11] T. Masuda and Y. Matsunaga, *Bull. Chem. Soc. Jpn.*, **64**, 2192, (1991).
- [12] M. Hird, Y. Raoul, J. W. Goodby and H. Gleeson, *Ferroelectrics*, **309**, 95, (2004).
- [13] M. Hird, J. Goodby, N. Gough, and K. J. Toyne, *J. Mater. Chem.* **11**, 2732, (2001).
- [14] S. Kang, Y. Saito, N. Watanabe, M. Tokita, Y. Takanishi, H. Takezoe and J. Watanabe, *J. Phys. Chem. B*, **110**, 5205, (2006).
- [15] W. Weissflog, U. Dunemann, S. F. Tandel, M. G. Tamba, H. Kresse, G. Pelzl, S. Diele, U. Baumeister, A. Eremin, S. Stern and R. Stannarius, *Soft Matter*, **5**, 1840, (2009).
- [16] U. Dunemann, M. W. Schroder, R. A. Reddy, G. Pelzl, S. Diele, W. Weissflog, *J. Mater. Chem.*, **15**, 4051, (2005).

- [17] G. Dantlgraber, D. Shen, S. Diele, C. Tschierske, *Chem. Mater.*, **14**, 1149, (2002).
- [18] D. Shen, A. Pegenau, S. Diele, I. Wirth, C. Tschierske, *J. Am. Chem. Soc.*, **122**, 1593, (2000).
- [19] D. Shen, S. Diele, G. Pelz, I. Wirth, C. Tschierske, *J. Mater. Chem.*, **9**, 661, (1999).
- [20] W. Weissflog, L. Kovalenko, I. Wirth, S. Diele, G. Pelzl, H. Schmalfuss, H. Kresse, *Liq. Cryst.*, **27**, 677, (2000).
- [21] H. T. Nguyen, J. C. Rouillon, J. P. Marcerou, J. P. Bedel, P. Barois, S. Sarmiento, *Mol. Cryst. Liq. Cryst.*, **328**, 177, (1999).
- [22] W. Weissflog, H. Nadasi, U. Dunemann, U. Pelzl, S. Diele, A. Eremin, H. Kresse, *J. Mater. Chem.*, **11**, 2748, (2001).
- [23] G. Pelzl, S. Diele, S. Grande, A. Jakli, C. Lischka, H. Kresse, H. Schmalfuss, I. Wirth, W. Weissflog, *Liq. Cryst.*, **26**, 401, (1999).
- [24] S. Shubashree, B. K. Sadashiva, S. Dhara, *Liq. Cryst.*, **29**, 789, (2002).
- [25] I. Wirth, S. Diele, A. Eremin, G. Pelzl, L. Kovalenko, N. Pancenko, S. Grande, W. Weissflog, *J. Mater. Chem.*, **11**, 1642, (2001).
- [26] W. Weissflog, Ch. Lischka, I. Benne, T. Scharf, G. Pelzl, S. Diele, H. Kruth, *Proc. SPIE*, **14**, 3319, (1998).
- [27] G. Pelzl, M.W. Schroder, U. Dunemann, S. Diele, W. Weissflog, C. Jones, D. Coleman, N.A. Clark, R. Stannarius, J. Li, B. Das, S. Grande, *J. Mater. Chem.*, **14**, 2492, (2004).
- [28] H. Nadasi, W. Weissflog, A. Eremin, G. Pelzl, S. Diele, B. Das, S. Grande, *J. Mater. Chem.*, **12**, 1316, (2002).
- [29] R. A. Reddy, B. K. Sadashiva, *J. Mater. Chem.*, **14**, 1936, (2004).
- [30] H. N. S. Murthy, B. K. Sadashiva, *J. Mater. Chem.*, **14**, 2813, (2004).
- [31] C. V. Yelamaggad, I. S. Shashikala, U. S. Hiremath, G. Liao, A. Jakli, D. S. S. Rao, S. K. Prasad, Q. Li, *Soft Matter*, **2**, 785, (2006).
- [32] B. E. Smart, *In Organofluorine Chemistry Principles and Commercial Applications*, R. E. Banks, B. E. Smart, and J.C. Tatlow, Eds.; Plenum Press: New York, p. **57**, (1994).
- [33] F. Guittard, S. J. Geribaldi, *Fluorine Chem.*, **107**, 363, (2001).

- [34] F. Guittard, E.T. deGivenchy, S. Geribaldi, A. J. Cambon, *Fluorine Chem.*, **100**, 85, (1999).
- [35] G. Pelzl, S. Diele, A. Jákli, C. Lischka, I. Wirth, and W. Weissflog, *Liq. Cryst.*, **26**, 135, (1999).
- [36] D. A. Coleman, J. Fernsler, N. Chattham, M. Nakata, Y. Takanishi, E. Křorblova, D. R. Link, R. F. Shao, W. G. Jang, J. E. Maclellan, O. M. Monval, C. Boyer, W. Weissflog, G. Pelzl, L. C. Chien, D. M. Walba, J. Zasadzinski, J. Watanabe, H. Takezoe and N. A. Clark, *Science*, **301**, 1204–1211, (2003).
- [37] H. N. S. Murthy, B. K. Sadashiva *Liq. Cryst.*, **30**, 1051, (2003).
- [38] A. Jakli, Ch. Lischka, W. Weissflog, G. Pelzl and A. Saupe, *Liq. Cryst.*, **27**, 1405–1409, (2000).
- [39] Gaussian 09, Revision B.01, M. J. Frisch, G. W. Trucks, H. B. Schlegel, G. E. Scuseria, M. A. Robb, J. R. Cheeseman, G. Scalmani, V. Barone, B. Mennucci, G. A. Petersson, H. Nakatsuji, M. Caricato, X. Li, H. P. Hratchian, A. F. Izmaylov, J. Bloino, G. Zheng, J. L. Sonnenberg, M. Hada, M. Ehara, K. Toyota, R. Fukuda, J. Hasegawa, M. Ishida, T. Nakajima, Y. Honda, O. Kitao, H. Nakai, T. Vreven, J. A. Montgomery, Jr., J. E. Peralta, F. Ogliaro, M. Bearpark, J. J. Heyd, E. Brothers, K. N. Kudin, V. N. Staroverov, T. Keith, R. Kobayashi, J. Normand, K. Raghavachari, A. Rendell, J. C. Burant, S. S. Iyengar, J. Tomasi, M. Cossi, N. Rega, J. M. Millam, M. Klene, J. E. Knox, J. B. Cross, V. Bakken, C. Adamo, J. Jaramillo, R. Gomperts, R. E. Stratmann, O. Yazyev, A. J. Austin, R. Cammi, C. Pomelli, J. W. Ochters R. L. Martin, K. Morokuma, V. G. Zakrzewski, G. A. Voth, P. Salvador, J. J. Dannenberg, S. Dapprich, A. D. Daniels, O. Farkas, J. B. Foresman, J. V. Ortiz, J. Cioslowski, and D. J. Fox, Gaussian, Inc., Wallingford CT, (2010).
- [40] K. Kim and K. D. Jordan "Comparison of Density Functional and MP2 Calculations on the Water Monomer and Dimer". *J. Phys. Chem.* **98**, **40**, 10089 (1994).
- [41] P.J. Stephens, F. J. Devlin, C. F. Chabalowski and M. J. Frisch "Ab Initio Calculation of Vibrational Absorption and Circular Dichroism Spectra Using Density Functional Force Fields". *J. Phys. Chem.* **98**, **45**, 11623 (1994).
- [42] K.H. Kim, Y.K. Han, J. Jung. *Theor. Chem. Acc.*, **113**, 233 (2005).
- [43] J. Aihara. *J. Phys. Chem. A*, **103**, 7487 (1999).
- [44] G. Pelzl, S. Diele, M. W. Schröder, W. Weissflog, M. G. Tamba, U. Baumeister, *Liquid Crystal*, **37**, 839- 852, (2010).